Biophys Struct Mech (1982) 9:35–60

Biophysics of Structure and Mechanism

The Gating of Single Calcium-Dependent Potassium Channels Is Described by an Activation/Blockade Mechanism

C. Methfessel and G. Boheim

Department of Cell Physiology, Ruhr-Universität Bochum,
Postfach 102148, D-4630 Bochum, Federal Republic of Germany

Abstract. Single calcium dependent potassium channels from cultured rat myoballs have been studied with the patch clamp technique, and current records subjected to statistical analysis. From the dependence of the mean open state probability on the internal calcium concentration, two calcium ions are required to open the channel. The open state and closed state lifetime distributions reveal that the usual activation model is not applicable to these channels. They are consistent with a two step gating mechanism that involves both activation by calcium and blockade by a calcium-sensitive gate.

Key words: Single channel currents – Channel activation – Channel blockade – Potassium channel – Calcium dependent channel

Introduction

It is well established that Ca^{2+} dependent K^+ currents occur in a wide variety of cell membranes (Meech 1978; Schwarz and Passow 1983). Recent work (Fink et al. 1983) has shown that the potassium outward current of exhausted muscle fibres is controlled by the internal calcium concentration.

Since the development of the patch clamp technique (Neher et al. 1978; Hamill et al. 1981), several investigators have reported Ca^{2+} dependent K^+ channels from various preparations, such as cultured bovine chromaffine cells (Marty 1981), Helix neurones (Lux et al. 1981), rat myotubes (Palotta et al. 1981; Barrett et al. 1982) and cultured bullfrog ganglion cells (Adams et al. 1982). Such channels have also been studied in rabbit T-tubule membrane fragments reconstituted into planar lipid bilayers (Latorre et al. 1982). In each case, the channels show a remarkably large conductance, yet are highly selective for K^+. Their opening frequency and lifetime clearly depend on both voltage and the internal Ca^{2+} concentration, but apparently in a complex way which still remains to be fully understood.

0340-1057/82/0009/0035/$ 05.20

We have recorded current fluctuations of a channel of this type from excised membrane patches taken from cultured rat myoballs, using the patch clamp technique as described by Hamill et al. (1981), and performed a statistical analysis of the single channel current fluctuations. To account for the dependence of the mean open and closed state lifetimes on the membrane potential and calcium concentration, a gating mechanism which involves both activation and blockade is proposed.

Theory

The switching properties of ion channels are usually discussed in terms of chemical thermodynamics and rate theory. The channel forming molecules are treated as chemical species that undergo monomolecular reactions, such as transformation into the open state, or bimolecular reactions, such as binding of an agonist. This is the reasonable approach when dealing with large numbers of channels that are not resolved individually, as in classical voltage clamp experiments. The measured membrane currents are related to the concentration of open channels in a straightforward way. With the patch clamp technique, however, individual ion channel currents are easily resolved and the number of channels studied in an experiment is ideally one, or as a rule at least very small. Under these conditions, it becomes somewhat artificial to speak of a 'concentration' of open or closed channels. Instead, the amount of time that the single ion channel spends in its various states becomes the quantity of interest, and it is more appropriate to use a statistical approach.

Statistical Description of Ion Channels

The basic assumption underlying a statistical discussion of ion channel kinetics is that the channel at any time is found in one of several permissible states, some of which are electrically conducting or open states and some of which are nonconducting or closed, and that it can undergo transitions between those states, with transitions between open and closed states observable as discrete electric current fluctuations. The transition rates may depend on external parameters such as voltage or chemical concentrations, but are assumed to be independent of the channel's past history and of time. Therefore, the correct mathematical description is in terms of a Markov process in continuous time (Colquhoun and Hawkes 1977), although an approximation by a Markov chain in discrete time (Kemeny and Snell 1976) may be more convenient, particularly if the data have been digitized for computer analysis.

The mathematical description of an ion channel is, then, as follows. The channel has k allowed states R_i denoted by indices $i = 1, 2, \ldots, k$. $P_i(t)$ is the probability of finding the channel in state i at time t. Since at any time the channel must be in one of its states,

$$\sum_{i=1}^{k} P_i(t) = 1 \qquad \text{for all } t\,. \tag{1}$$

The transition rate from one state R_i to another state R_j is denoted by λ_{ij}.

If the probabilities $P_i(t)$ are regarded as a k-dimensional vector

$$\vec{P}(t) = [P_1(t), P_2(t), \ldots, P_k(t)] \tag{2}$$

and the transition rates as a $k \cdot k$ matrix,

$$\Lambda = \begin{pmatrix} \lambda_{11} \ldots\ldots \lambda_{1k} \\ \vdots \qquad\quad \vdots \\ \lambda_{k1} \ldots\ldots \lambda_{kk} \end{pmatrix} \tag{3}$$

the temporal evolution of the system is described by the vector equation

$$\frac{d\vec{P}(t)}{dt} = \vec{P}(t) \cdot \Lambda \tag{4}$$

which is sometimes referred to as the Master equation. It is a system of k coupled linear differential equations

$$\dot{P}_i(t) = \sum_{j=1}^{k} P_j(t)\, \lambda_{ji} \,. \tag{5}$$

If a transition between two states cannot occur for any reason, the corresponding transition rate of course is zero. Therefore, the analysis can be simplified by uncoupling the differential equations through restrictions on the possible transitions (Neher and Steinbach 1978). For example, in a linear reaction scheme

$$R_1 \rightleftharpoons R_2 \rightleftharpoons R_3 \rightleftharpoons \ldots . \rightleftharpoons R_k, \tag{6}$$

from state i only transitions to states $i+1$ and $i-1$ are allowed. This simplifies the differential eq. (5) into the form

$$\dot{P}_i(t) = \lambda_{i-1,i}\, P_{i-1}(t) - (\lambda_{i,i-1} + \lambda_{i,i+1})\, P_i(t) + \lambda_{i+1,i}\, P_{i+1}(t) \,. \tag{7}$$

Generally, one is interested in the mean lifetime of the channel states. Suppose that the channel is known to be in a given state i at time $t = 0$ (for example, at the moment when the channel opens it is known to be in the open state). Then, $P_i(0) = 1$. By setting all transition rates into the open state to zero, the probability that the channel is still open at a later time t is

$$P_i(t) = \exp(-t/\tau_i) \,, \tag{8}$$

where

$$\tau_i = (\lambda_{i,i-1} + \lambda_{i,i+1})^{-1} \tag{9}$$

is the mean lifetime of the channel state i.

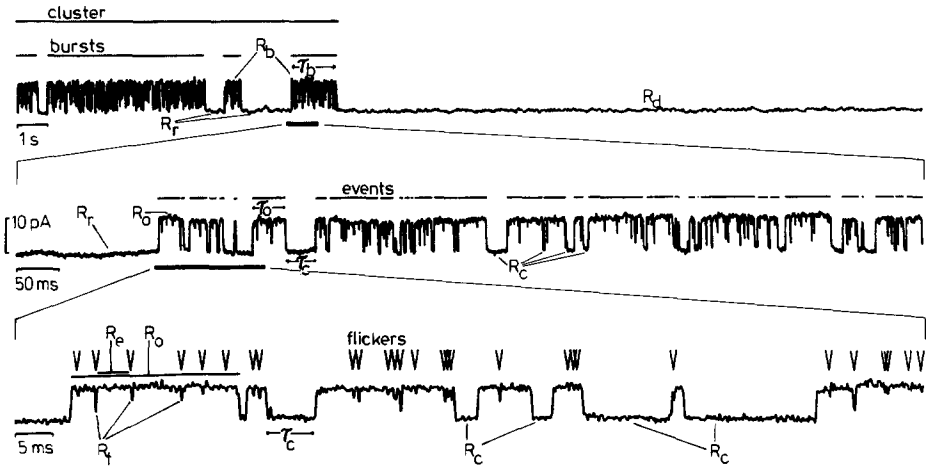

Fig. 1. Typical current fluctuations from a membrane patch containing one Ca^{2+} dependent K^+ channel recorded at +40 mV. Experimental conditions are identical with Fig. 5a. Top trace: Viewed over a long time, the channel shows bursts of activity that themselves occur in clusters. After depolarization to +40 mV the channel usually starts out in the bursting mode and after a while desensitization sets in. Middle trace: At a somewhat faster time resolution, the bursts are resolved into individual open and closed state events. Bottom trace: at even faster time resolution, brief flickers are seen which are too rapid to be resolved fully with the equipment used. The various states of the channel are labelled as described in the text

A typical ion channel will usually have more than two states. For example, as illustrated in Fig. 1, the Ca^{2+} dependent K^+ channel can enter at least five different states, and a complete description of the channel must consider them all. However, actual statistical analysis for a large number of states could be quite cumbersome. Also, not all of the states may be easily accessible to measurement. Some states may be too short-lived to be resolved clearly in an experiment, while others may be too infrequent or too persistent to allow enough data to accumulate in a reasonable amount of time.

It is possible to group together any two or more adjacent states into one state. The channel is considered to be in this group state as long as it is in any one of the actual states comprised in the group, and transition rates are defined into and out of this group state. If transition rates within the group are much larger than those to states outside the group, then such a group state behaves exactly like a true channel state. At several points in our analysis we make use of this statistical property.

States of the Ca^{2+} Dependent K^+ Channel

Figure 1 shows a typical current fluctuation recorded at +40 mV from a membrane patch containing one Ca^{2+} dependent K^+ channel. It exhibits several kinds of closures, as distinguished by their mean duration, which resemble those presented by the acetylcholine receptor under desensitizing concentrations of

agonist (Sakmann et al. 1980) so closely that the same terminology seems applicable. We consider the current fluctuations resolved in the center trace to represent the channel's transition between the closed and open states. Viewing a longer segment of the record, one readily sees that the channel activity occurs in 'bursts' separated by quiet periods. Moreover, the bursts do not appear singly but in 'clusters' separated by even longer silent intervals, up to minutes in duration. After depolarizing shifts in potential, the channels frequently are active for several seconds before desensitization sets in. On a much faster time scale, the open state 'events' themselves are frequently interrupted by closures which usually are too short to resolve clearly. These 'flickers' or 'closing gaps' are a general feature of ion channels (see for example Colquhoun and Sakmann 1981; Cull-Candy and Parker 1982), but here they appear to be especially pronounced. We identify the various channel states by the following subscripts, as shown in Fig. 1: The electrically conducting state is called R_e. Of the closed states, R_c means the channel closures between the open events, R_f corresponds to the brief closing gaps or flickers, R_r refers to the 'resting' state between bursts, and R_d denotes the long desensitized period between clusters. It is unlikely that this listing includes all of the states that the Ca^{2+} dependent K^+ channel can adopt. Indeed, Barrett et al. (1982) describe a second open state of shorter lifetime, comparable to that of the closing gaps, as well as an intermediate state with about 40% of the full channel conductance. We have also seen both of these states, as well as partial closures to values other than 40% of the full conductance. However, they are too infrequent in our records for inclusion in the statistical analysis at the present time.

It has become apparent that a full description of these channels will be rather complicated, since it must involve the electrically conducting state and at least four different closed states, with transition rates that may depend both on the membrane potential and on the calcium concentration. In the present analysis we have therefore restricted ourselves to the open events, and to the closures separating them, within the bursts. We do not analyze the behaviour of the bursts and the clusters, and also ignore the flickering of the open channels. This means that we are grouping together, as described above, the electrically conducting state R_e and the very briefly closed flicker state R_f into one state, which we call the open state, R_o. Because we do not discuss the lifetimes of the R_r and R_d states, it is convenient to consider them together as a 'silent' state, R_s. Thus we are discussing below a simplified system of only three states: the open state R_o, the closed state R_c, and the silent state R_s.

Models for the Channel

a. Activation Model. The simplest model that we wish to consider is that of an ordinary agonist-activated channel, as it is generally assumed for the acetylcholine receptor channel (e.g., Adams 1981) and has been proposed for the Ca^{2+} dependent K^+ channel of rabbit T-tubuli by Latorre et al. (1982). This model suggests itself through the observation that under normal conditions channel activity appears to be increased with intracellular calcium. We postulate

that two calcium ions must bind to open the channel because, as will be seen below, this agrees best with our own and with other data (Latorre et al. 1982; Barrett et al. 1982). Moreover, for many other agonist activated channels, such as the acetylcholine receptor channel (Adams 1981) and the glycine and glutamate receptors from spinal neuron cells (Sakmann et al. 1982), two agonist molecules apparently are required for activation to occur. The reaction scheme is

$$\begin{aligned} &Ca^{2+} + R_t \overset{M_1}{\rightleftharpoons} R_1 , \qquad Ca^{2+} + R_1 \overset{M_2}{\rightleftharpoons} R_2 , \\ &R_2 \underset{\lambda_{o2}}{\overset{\lambda_{2o}}{\rightleftharpoons}} R_o \underset{\lambda_{so}}{\overset{\lambda_{os}}{\rightleftharpoons}} R_s , \end{aligned} \tag{10}$$

where R_t, R_1, and R_2 denote the closed channel with no, one, and two bound calcium ions, respectively. Note that the channel must pass through three nonconducting states before opening. However, since they are electrically indistinguishable, it is reasonable to group them all together into one closed state, R_c:

$$2\ Ca^{2+} + R_c \underset{\lambda_{oc}}{\overset{\lambda_{co}}{\rightleftharpoons}} R_o \underset{\lambda_{so}}{\overset{\lambda_{os}}{\rightleftharpoons}} R_s . \tag{11}$$

If we assume that the transition rates of calcium binding and dissociation are very large compared to the transition rate of channel opening, there will be a stationary distribution of the closed channel into the states R_t, R_1 and R_2. Accordingly for the closed state R_c

$$P_c = P_t + P_1 + P_2 = \left(1 + \frac{M_2}{[Ca^{2+}]} + \frac{M_1 \cdot M_2}{[Ca^{2+}]^2}\right) P_2 , \tag{12}$$

where M_1 and M_2 are the corresponding equilibrium constants of the channel binding sites for calcium.

The transition rate from the combined closed state into the open state is

$$\lambda_{co} = \frac{\lambda_{2o}}{\left(1 + \frac{M_2}{[Ca^{2+}]} + \frac{M_1 \cdot M_2}{[Ca^{2+}]^2}\right)} . \tag{13}$$

Assuming low affinity binding constants ($M_1 \gtrsim 10^{-4}$ M, $M_2 \gtrsim 10^{-4}$ M) and Ca^{2+} concentrations around 1 μM this expression is simplified to

$$\lambda_{co} = \lambda_{2o} \cdot \frac{[Ca^{2+}]^2}{M_1 \cdot M_2} . \tag{14}$$

Thus for the closed state, R_c, (Eq. 7) is

$$\dot{P}_c(t) = -\frac{[Ca^{2+}]^2}{M_1 \cdot M_2} \lambda_{2o} P_c(t) + \lambda_{o2} P_o(t) \tag{15}$$

and from the corresponding decay law we get the mean lifetime of the closed events

$$\tau_c = \frac{M_1 \cdot M_2}{\lambda_{2o}\,[Ca^{2+}]^2}\,. \tag{16}$$

For the open state probability $P_o(t)$ we have the expression

$$\dot{P}_o(t) - \lambda_{co}\,P_c(t) + \lambda_{so}\,P_s(t) - (\lambda_{oc} + \lambda_{os})\,P_o(t)\,. \tag{17}$$

If we restrict ourselves to evaluating only within the bursts, the transition rates to and from R_s may be considered zero and the mean lifetime of the open states becomes

$$\tau_o = \frac{1}{\lambda_{oc}}\,. \tag{18}$$

This approximation is valid if the burst duration τ_b is much larger than the lifetimes of individual events and closures τ_o and τ_c (see Fig. 1).

Therefore, the activation model predicts a duration of closures that decreases with increasing calcium concentration with an exponent reflecting the number of calcium ions that must bind before opening, and a duration of openings that is independent of agonist concentration. The equilibrium constant between the open and closed states within the bursts becomes

$$K = \frac{\lambda_{co}}{\lambda_{oc}} = \frac{\tau_o}{\tau_c} \sim [Ca^{2+}]^2 \tag{19}$$

over the corresponding range of Ca^{2+} concentrations.

b. Blockade Model. Another model for the kinetics of these channels was recently discussed (Boheim et al. 1982) to account for the distinct dependence of the open lifetimes on the calcium concentration and to plausibly explain the close correlation between the effects of voltage and calcium on the channels. This model assumes a negatively charged 'gate' or plug, which blocks the channel under normal conditions from the inside. There is a voltage-dependent probability, which increases with more positive (inside) potentials, for the gate to leave the channel and thus open it. In this unblocked state, calcium can bind to the gate and neutralize its charge. Then the channel stays open, since the neutralized gate, G_o, cannot exert the blocking action. The open channel may then go into the desensitized state. The reaction scheme for this model is

$$R_c \underset{\lambda_{oc}}{\overset{\lambda_{co}}{\rightleftharpoons}} R_o + G^{4-} \qquad R_o \underset{\lambda_{so}}{\overset{\lambda_{os}}{\rightleftharpoons}} R_s\,,$$

$$G^{4-} + Ca^{2+} \overset{L_1}{\rightleftharpoons} G^{2-} \qquad G^{2-} + Ca^{2+} \overset{L_2}{\rightleftharpoons} G_o\,. \tag{20}$$

The transition rates of binding and dissociation again are assumed to be large compared to those of the other steps. Whereas in the absence of Ca^{2+} the dissociated gate is continuously available to react with the channel again ($\bar{P}_G = 1$), in the presence of Ca^{2+} the availability of the gate is reduced to

$$\bar{P}_G = \frac{1}{1 + \frac{[Ca^{2+}]}{L_1} + \frac{[Ca^{2+}]^2}{L_1 \cdot L_2}}, \tag{21}$$

where L_1 and L_2 are the two binding constants of the gate for calcium. For the closed state, we have

$$\dot{P}_c(t) = -\lambda_{co}\, P_o(t) + \lambda_{oc}\, \bar{P}_G\, P_o(t), \tag{22}$$

and its mean lifetime is given by

$$\tau_c = \frac{1}{\lambda_{co}}. \tag{23}$$

The expression for the open state is again more complicated due to the silent state

$$\dot{P}_o(t) = \lambda_{co}\, P_c(t) - \lambda_{oc}\, \bar{P}_G P_o(t) - \lambda_{os}\, P_o(t) + \lambda_{so}\, P_s(t), \tag{24}$$

but can be approximated as before for the case of evaluation only within long bursts by

$$\dot{P}_o(t) = \lambda_{co}\, P_c(t) - \lambda_{oc}\, \bar{P}_G P_o(t), \tag{25}$$

from which the mean open time follows:

$$\tau_o = \frac{1}{\lambda_{oc}\, \bar{P}_G} = \frac{1}{\lambda_{oc}} \left(1 + \frac{[Ca^{2+}]}{L_1} + \frac{[Ca^{2+}]^2}{L_1 \cdot L_2}\right). \tag{26}$$

Assuming high affinity binding constants ($L_1 \lesssim 10^{-7}$ M, $L_2 \lesssim 10^{-7}$ M) and Ca^{2+}-concentrations $\gtrsim 1$ μM this expression reduces to

$$\tau_o = \frac{[Ca^{2+}]^2}{\lambda_{oc} \cdot L_1 \cdot L_2}. \tag{27}$$

The equilibrium constant between the open and closed states is

$$K = \frac{\lambda_{co}}{\lambda_{oc}\, \bar{P}_G} = \frac{\tau_o}{\tau_c} \sim [Ca^{2+}]^2 \tag{28}$$

which is proportional to $[Ca^{2+}]^2$ within the range of the approximation. Note that the same dependence was found for the activation model (Eq. 19). However, in the blockade model one expects the closed intervals between openings to be independent of $[Ca^{2+}]$, and open lifetimes to depend on $[Ca^{2+}]^2$ for higher values of calcium. For $[Ca^{2+}]^2$ below the binding constants of the gate τ_o and K should become independent of $[Ca^{2+}]$.

Note that this model predicts a close coupling between the effects of calcium and of membrane potential. The mechanism of the transition between the open and closed states is the plugging of the channel by the free gate. Therefore the ratio $\lambda_{co}/\lambda_{oc}$ determines the distribution of charged gate outside and inside of the channel, which depends on the membrane potential

$$\frac{\lambda_{co}}{\lambda_{oc}} = \exp\left[\frac{n \cdot |z| \cdot F}{RT} \cdot (V - V^*)\right], \tag{29}$$

where R is the gas constant, F the Faraday constant, T the absolute temperature and z the charge on the gate. V^* is the reference voltage where $\lambda_{co} = \lambda_{oc}$, and n indicates how much of the membrane potential is seen by the gate during the gating process. In accordance with the experimental results that the potential dependence of K yields $n \cdot |z| = 2$ and that two Ca^{2+} ions should bind to the gate, we assign $z = -4$ and $n = 0.5$. For the range of approximation $[Ca^{2+}] > L_1, L_2$, the equivalence relation between potential and $[Ca^{2+}]$ is

$$\Delta V = V_2 - V_1 = \frac{2 \cdot RT}{n \cdot |z| \cdot F} \ln \frac{[Ca^{2+}]_1}{[Ca^{2+}]_2}. \tag{30}$$

c. Activation/Blockade Model. We now propose a third model which combines some features from each of the preceding ones. We assume a ligand binding step in which one calcium ion is bound to a negatively charged binding site, presumably near the intracellular entrance of the channel, putting the channel into an active configuration. However, this active channel is still nonconducting because of the negatively charged gate blocking it. As in the second model, the gate can be withdrawn by a sufficiently positive membrane potential and neutralized by an additional calcium ion to free the channel for conduction. In view of the two other models a and b, this implies the existence of one high affinity and one low affinity binding site. If the low affinity site is not occupied, its negative charge will drive the gate into the channel. The gate is therefore locked into the channel by the mutual repulsion of the negatively charged binding sites. The probability that the gate opens the channel by leaving it is therefore much higher when the entrance charges associated with the low affinity site are neutralized by Ca^{2+}. We thus propose the reaction scheme

$$Ca^{2+} + R_t \overset{M}{\rightleftharpoons} R_1 \underset{\lambda_{o1}}{\overset{\lambda_{1o}}{\rightleftharpoons}} R_o + G^{2-}, \qquad R_o \underset{\lambda_{so}}{\overset{\lambda_{os}}{\rightleftharpoons}} R_s,$$
$$Ca^{2+} + G^{2-} \overset{L}{\rightleftharpoons} G_o. \tag{31}$$

Again we assume that the transition rates of calcium binding and dissociation are large compared to all other transition rates so that the calcium dependent probability for the presence of the closed state R_c is given by

$$P_c = P_t + P_1 = P_1 \cdot \left(1 + \frac{M}{[Ca^{2+}]}\right), \tag{32}$$

and the availability of the free gate is reduced to

$$\bar{P}_G = \frac{1}{1 + \dfrac{[Ca^{2+}]}{L}}, \tag{33}$$

where M and L are the calcium binding constants of the channel and the gate, respectively. Since we cannot distinguish electrically between the state of the channel with and without calcium, we have grouped them together as before into the closed state, labeled R_c. In Eq. (32), P_1 and P_c are proportional and the Master equation for the closed state R_c becomes

$$\dot{P}_c(t) = \left(1 + \frac{M}{[Ca^{2+}]}\right) \cdot \dot{P}_1(t) = -\lambda_{1o} P_1(t) + \lambda_{o1} \bar{P}_G P_o(t), \tag{34}$$

from which the mean lifetime for this state becomes

$$\tau_c = 1/\lambda_{1o} \cdot \left(1 + \frac{M}{[Ca^{2+}]}\right). \tag{35}$$

The differential equation for the open state R_o is

$$\dot{P}_o(t) = \lambda_{1o} P_1(t) - (\lambda_{o1} \bar{P}_G + \lambda_{os}) P_o(t) + \lambda_{so} P_s(t). \tag{36}$$

With the same assumptions as before, the mean lifetime for the open state within a burst is

$$\tau_o = \frac{1}{\lambda_{o1} \bar{P}_G} = \frac{1}{\lambda_{o1}} \cdot \left(1 + \frac{[Ca^{2+}]}{L}\right). \tag{37}$$

The equilibrium constant for the opening and closing of channels within bursts is then

$$K = \frac{T_o}{T_c} = \frac{\lambda_{1o}}{\lambda_{01}} \cdot \frac{1 + [Ca^{2+}]/L}{1 + M/[Ca^{2+}]}. \tag{38}$$

If the channel receptor site is of low affinity ($M \gtrsim 10^{-4}$ M), but the gate itself has a high affinity for calcium ($L \lesssim 10^{-7}$ M), then the apparent equilibrium constant between the open and closed states will be approximated at $[Ca^{2+}] \gtrsim 1$ μM by

$$K \approx \frac{\lambda_{1o}}{\lambda_{o1}} \cdot \frac{[Ca^{2+}]^2}{LM} \sim [Ca^{2+}]^2. \tag{39}$$

Whereas for $[Ca^{2+}] \gtrsim 1$ μM the apparent equilibrium constant K shows the same dependence on $[Ca^{2+}]$ for all three models, the activation/blockade model differs from the others in predicting that the open and closed state lifetimes should *both* depend on the calcium concentration.

The three models can therefore be distinguished on the basis of the τ_o and τ_c data, and of K at Ca^{2+} concentrations below the binding constant of the high affinity site postulated by us ($[Ca^{2+}] < 10^{-7}$ M).

The voltage dependence of channel gating is described in terms of the model c by

$$\frac{\lambda_{1o}}{\lambda_{o1}} = \exp\left[\frac{|z| \cdot F}{RT}(V - V^*)\right], \tag{40}$$

with $z=-2$, since the gate binds only one calcium ion. Taking this z-value and Eq. (40), the equivalence relation for voltage and $[Ca^{2+}]$ becomes

$$\Delta V = \frac{RT}{F} \cdot \ln \frac{[Ca^{2+}]_1}{[Ca^{2+}]_2} \tag{41}$$

which, of course, is the same as obtained for model b (Eq. 30).

Concerning the mean duration of the bursts τ_b, we can write down a relation under the assumption that the channel inactivates only from the open state, as suggested by the linear reaction scheme and in analogy to the acetylcholine receptor in the presence of certain drugs (Neher and Steinbach 1978). Then τ_b should depend on the apparent equilibrium constant $K(V, [Ca^{2+}])$ and the transition rate λ_{os} in the following way:

$$\tau_b = \frac{1}{\lambda_{os}} \cdot (1 + 1/K) . \tag{42}$$

This expression holds for all three models. Changing membrane voltage to more positive values or increasing the Ca^{2+} concentration in each case leads to shorter burst durations. A qualitative inspection of the experimental data shows that this, indeed, occurs.

Materials and Methods

Experimental

Single channel current fluctuations from Ca^{2+} dependent K^+ channels were recorded from rat myoballs using the patch clamp technique (Hamill et al. 1981). In the work reported here, we have used the outside-out patch configuration. After gigaseal formation the first (on cell) patch is destroyed by suction and the pipette is then withdrawn, together with a small amount of membrane which reseals after separating from the cell. In this way a closed, isolated patch of membrane is obtained with its intracellular side exposed to the pipette solution and its outside facing the external bathing solution.

Pipettes were filled with 150 mM KCl buffered with 3 mM HEPES-KOH to pH 7.2. In the outside-out patch configuration, this becomes the inside solution. To obtain defined calcium concentrations, solutions containing 1 mM EGTA and an amount of calcium calculated to give the desired level of free Ca^{2+} ions were prepared as shown in Table 1.

The outside bath solution was a sodium Ringe's solution containing 150 mM NaCl, 4 mM KCl, 1 mM $CaCl_2$ and 1 mM $MgCl_2$, or a potassium bath solution containing 150 mM KCl, 4 mM NaCl, 3 mM $CaCl_2$, and 1 mM $MgCl_2$. The higher

Table 1. Free calcium concentrations were calculated using an apparent dissociation constant for Ca^{2+}-EGTA of $4.83 \cdot 10^6$ M^{-1} (Hagiwara and Nakajima 1966)

Nominal free Ca^{2+} [μM]	EGTA [μM]	$CaCl_2$ [μM]
2	1,000	900
1	1,000	830
0.05	1,000	200
0.001	1,000	≈ 5

calcium concentration was chosen to stabilize the membrane patches which otherwise tended to become leaky when exposed to a potassium rich bath with their outside face. The bath solutions were also buffered to pH 7.2 with 3 mM HEPES and NaOH or KOH, respectively. All salts used were of p.A. grade.

After a good outside-out patch clearly showing one or several channels was obtained, the bath was exchanged to the K^+ solution so that the channel's activity might be observed at all membrane potentials. Current signals were amplified with a patch clamp circuit as described (Hamill et al. 1981) and recorded on a Racal recorder. The bandwidth of the system was better than 2.5 kHz, and background noise usually less than 0.5 pA. Experiments were performed at a temperature of 18°–20° C.

Statistical Evaluation

The simplest statistical parameter that can be determined from a single channel recording is P_o, the long term average probability of finding the channel in the open state. This differs from $P_o(t)$ in being a stationary value meaningful only for a sufficiently long record, whereas $P_o(t)$ is the instantaneous value of the probability that the channel is open, which depends on the preceding states and therefore on time. In general, the value of P_o multiplied by the number of channels and by the single channel conductance corresponds to the macroscopic conductance measured in a classical voltage clamp preparation. In the case of the present channels, however, the situation is complicated by the effects of desensitization. Since the models proposed above do not differ in their predictions about P_o over the range of calcium concentrations studied, we also evaluated the mean open state lifetime τ_o and the mean closed interval lifetime τ_c from our records. The ratio of these two lifetimes, τ_o/τ_c, corresponds to the equilibrium constant of the two states of the channels under the assumption of no desensitization, i.e., within the bursts. The various quantities are related in the following way:

$$\mathrm{K} = \frac{\tau_o}{\tau_c} = \frac{P_o}{1 - P_o}; \qquad P_o = \frac{\tau_o}{\tau_o + \tau_c} = \frac{\mathrm{K}}{\mathrm{K} + 1}. \tag{43}$$

As shown below, the mean lifetimes τ_o, τ_c and the mean open state probability P_o can be determined separately, so that Eq. (43) gives a way of checking the

consistency of the statistical results obtained from a patch-clamp experiment.

Event lifetime, intervals, and the proportion of time in the open state were evaluated with the help of a computer program. The signals were replayed from the tape recorder into an analog/digital converter (Digital MNCAD11) at a sampling rate of 1,000 points per second. Sampling points with current values exceeding a given threshold were considered to represent the open state of the channel, and current values below the threshold were counted as closed. The threshold was usually set at the middle between the open and closed current levels. The number of data points between two successive crossings of the threshold was recorded as the duration of an open or closed event, respectively. In this way, a distribution of open and closed event lifetimes was obtained from which the mean lifetimes τ could be obtained with a simple exponential fit, done as linear regression on the logarithms.

Since we did not wish to include the flickering process in our analysis, we had to find a way to eliminate the brief flicker closures from our records before proceeding with the statistical evaluation. This was accomplished with a feature in the counting program that allowed setting a lower limit for the duration of the closures. Thus, all closures shorter than the limit were ignored and the entire sequence of openings between two closures exceeding the limit was counted as one open event. Figure 2 shows the effect of this procedure on the lifetime values returned by the computer program.

Although they too had to be excluded carefully from the analysis, the long silent intervals between the bursts and clusters presented much less of a problem. At higher calcium concentrations and potentials, the bursts were so clearly evident that evaluation could easily be restricted to within them (e.g., Fig. 1, or Fig. 5A at 60 and 80 mV). At lower $[Ca^{2+}]$ and potentials where the inter-burst interval lifetime might be comparable to that of the closed events, the burst lifetimes were so much longer than the individual open and closed state lifetimes that any error introduced was very small. However, under all conditions, any quiet periods that were very much longer than the typical closed events were considered to be silent intervals and not included in the determination of P_o. In the lifetime histograms used for the determination of the time constants, the ten most long-lived events were as a rule excluded from the fitting because, representing a very small sample, they scattered widely and tended to falsify the distribution given by the majority of events. This also insured that any long desensitized states were excluded. In addition to the evaluation of the event lifetime distributions, the mean open state probability P_o within the bursts was determined directly by simple counting of data points representing the open and closed states. Because of Eq. (43), this value can be used to check results for consistenty. It appears that P_o is much less variable from one experiment to another, or with time within one experiment, than the values obtained for the time constants. These values scatter more strongly, although in such a way that τ_o/τ_c remains constant. One reason for this may be that in contrast to τ_o, the value of P_o is not much affected by the presence of flickers because of their shortness. If the apparent equilibrium constant K, rather than the actual mean state lifetime, is of interest it is therefore more convenient to

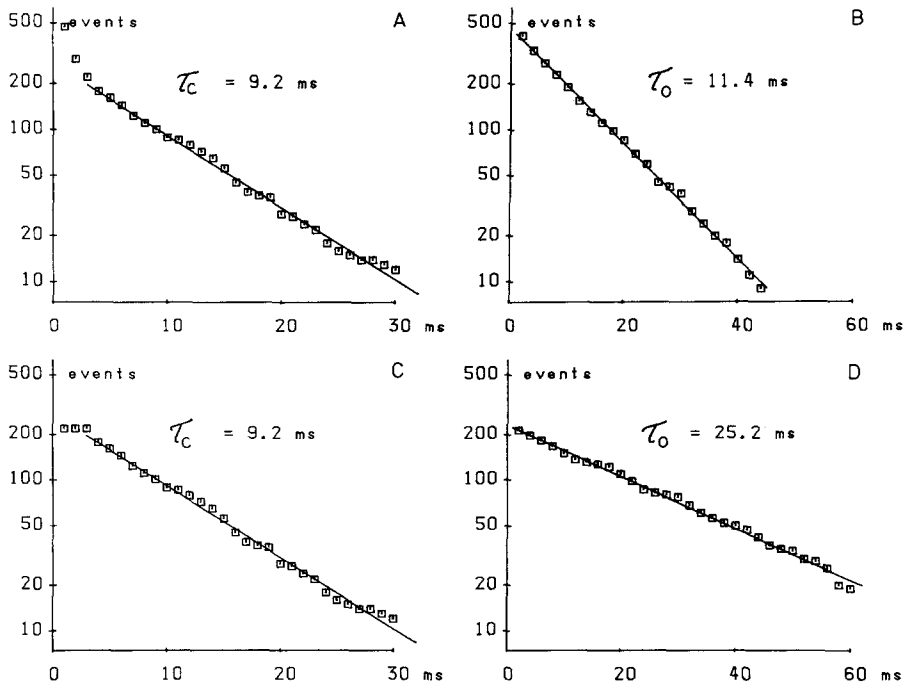

Fig. 2A–D. The effect of the brief 'flicker' closures on the open lifetime evaluation is shown. For the upper graphs (**A** and **B**) all closures resolved at a sampling rate of 1,000/s were counted. The closed event lifetime distribution (**A**) shows two time constants arising from the states R_c and R_f, respectively, and the correct value of the closed event time constant τ_c can be obtained easily from **A** if one is careful to exclude the first few points from the regression. But the value $\tau_o = 11.4$ ms found for the open states is wrong, because many of the open events were interrupted by flickers. For the lower graphs (**C** and **D**) only closures longer than 3 ms were counted and all shorter closures were ignored. The graph of the closed lifetime distribution is therefore truncated at 3 ms, which does not influence the value of τ_c. The open lifetime distribution, however, has changed drastically, giving $\tau_o = 25.2$ ms. This value is still in error by a small amount, because along with the flickers, a certain number of real closures shorter than 3 ms was eliminated (in principle, there may also be a few particularly long lived flicker states which are still included). This error is small if the mean lifetime of the closed states is much larger than that of the flicker states. The comparison of the extrapolated $N(0)$ values in (**C**, **D**) shows that this systematic error was at most 20% during our analysis. Note that any attempt to evaluate the lifetime of the actual conducting states, R_e, between the flicker closures is doomed to failure because the bandwidth of the apparatus does not allow proper resolution of the flicker states; any such attempt yields results only reflecting the rise time of the amplification circuitry. Such analyses would require much faster amplifiers capable of clearly resolving the flicker states. Data for these figures were taken from the same record as for Fig. 1

work with P_o. Note, however, that P_o is strongly affected by inadvertent inclusion of any long silent periods, so that in determining P_o one must be very careful to remain within the bursts.

In some experiments, two or more Ca^{2+} dependent K^+ channels were active in one membrane patch. In such cases, one of two methods was used depending on the type of fluctuations. Under conditions where the channels are bursting, it usually was no problem to find a section of the record in which all but one of the channels were in the silent state, so that evaluation could proceed normally for

the one active channel. At more negative potentials where the channels do not exhibit the silent state, the probabilities for the various current states, (e.g., for the case of two channels the states P_0 = all channels closed, P_1 = one channel open, and P_2 = both channels open) were determined by counting and fitted to a binomial distribution to obtain the open state probability P_o for one channel. The values P_o obtained in this way agreed well with those for experiments with only one channel. However, the lifetime histogram evaluation was not performed in the case of multiple channels.

Results

Figure 3a shows current fluctuations from a membrane patch containing one calcium dependent K^+ channel with sodium Ringer's solution in the outside bath. At voltages more negative than −60 mV, no events were detected. Due to the high selectivity of the channel, a large potassium outward current is found even at negative membrane potentials. Figure 3B shows that with the potassium bath solution outside similar current fluctuations are observed, but the reversal potential is now at zero millivolts and at negative potentials a potassium inward current is seen. From Fig. 3 it is obvious that the channel kinetics are voltage dependent, with both frequency and lifetime of events increasing with voltage. At positive potentials, however, additional long lived closed states let activity occur in bursts separated by long silent intervals, as was already shown in Fig. 1. This process is also voltage dependent, but in the opposite sense, so that the bursts become shorter, and the intervals between them longer, with increasing positive potential. Indeed, at higher positive potentials the duration of the bursts becomes so short that they, rather than the events, determine the appearance of the trace. At less positive potentials the burst lifetime becomes so long that the silent intervals are rarely seen at all.

Channel Conductance and Selectivity

Figure 4 shows the channel current as a function of applied membrane potential both with normal sodium Ringer's solution and with potassium bath solution outside. Under symmetric K^+, the channel obeys Ohm's law over a wide voltage range and has a conductance of 240 pS, which is high indeed for an ion channel. Assuming that the channel is impermeable to Cl^- as suggested strongly by Fig. 3 the selectivity ratio, $b = P_K/P_{Na}$, can be determined according to the Goldman equation (Katz 1966) from the reversal potential with Na^+ Ringer's solution outside,

$$E_{rev} = \frac{RT}{F} \cdot \ln \frac{b \cdot [K^+]_o + [Na^+]_o}{b \cdot [K^+]_i + [Na^+]_i} . \tag{44}$$

With $E_{rev} \approx -54$ mV the selectivity ratio is at least 15 : 1 and may be as high as 21 : 1. With 150 mM Cs^+ outside instead of Na^+, the selectivity is between 4 and 10 : 1. Since the concentration of Cl^- was the same in all solutions, it is safe to

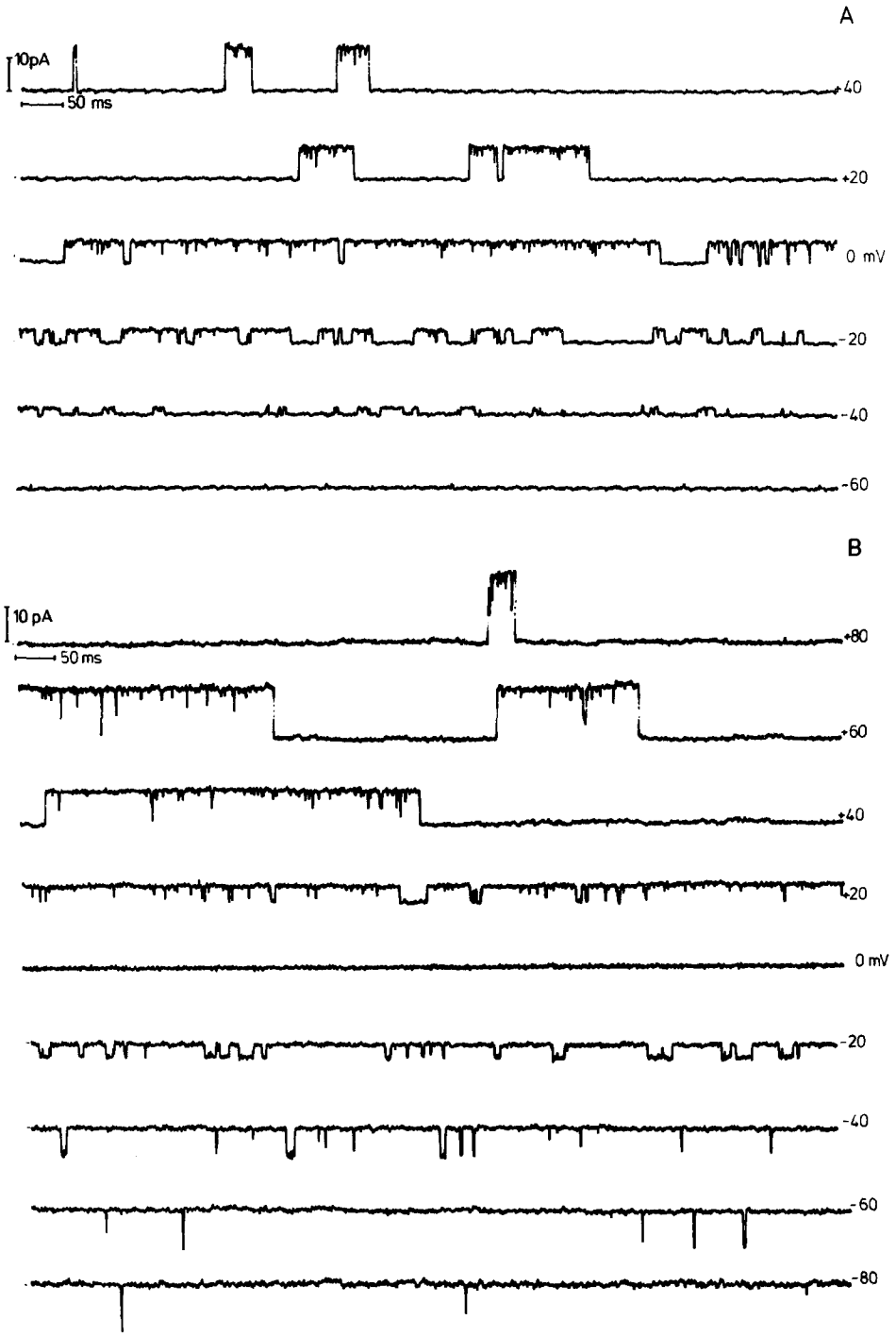

Fig. 3A and B. Current fluctuations recorded from an outside-out membrane patch containing one calcium dependent K^+ channel. Pipette solution: 150 mM KCl buffered to pH 7.3 with HEPES-KOH. No EGTA or calcium were added, so that the calcium concentration at the inside face of the membrane was at some low, but undefined level (estimate: 5 μM). Outside bath solution: **A,** sodium Ringer's solution, **B,** potassium bath solution (see 'materials' for details)

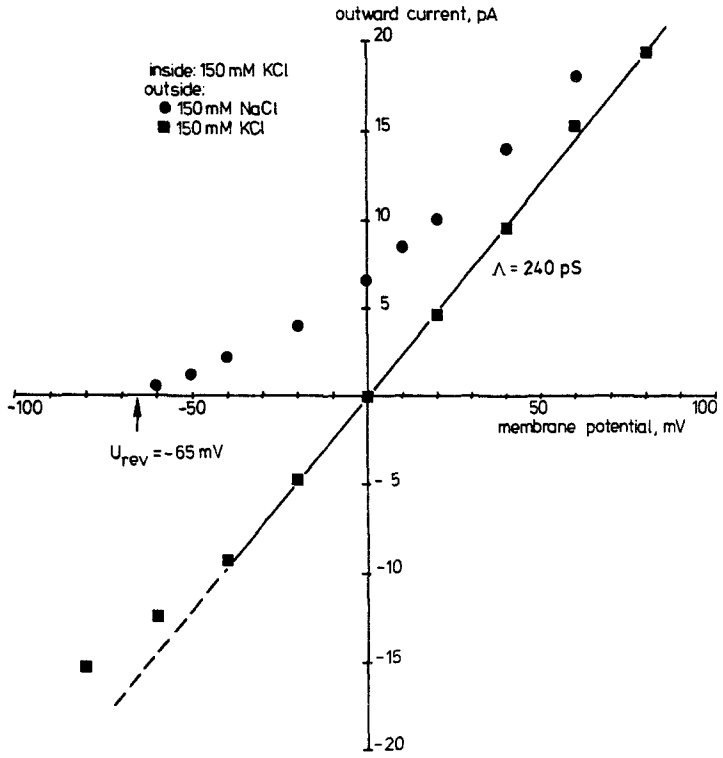

Fig. 4. Single channel current as a function of membrane potential for the open calcium dependent K^+ channel with sodium and potassium bath solutions outside. Experimental conditions as in Fig. 3. From the slope of the current-voltage relationship in symmetric K^+ the channel conductance of 240 pS is determined and from the curve with sodium Ringer's solution outside, the reversal potential of −65 mV is found

conclude that the permeating ion species for this channel is potassium, as is also indicated by the ability of 5 mM TEA to block the channels reversibly from the outside bath solution. It is an interesting observation that the conductance of these channels is not constant from one membrane patch to another, although it is quite constant for one experiment and always lies between 180 and 260 pS.

Effect of Calcium and of Membrane Potential

The records in Fig. 3 were obtained using a pipette filling solution to which no calcium or EGTA had been added, so that the concentration of calcium was presumably in the range of 5 μM due to background calcium in the water and p.A. grade salts used. In Fig. 5 the effect of a reduced inside calcium concentration on the channel is shown, recorded using pipettes filled with buffered Ca^{2+} concentrations of Table 1. Fluctuations seen at internal $[Ca^{2+}]$ of

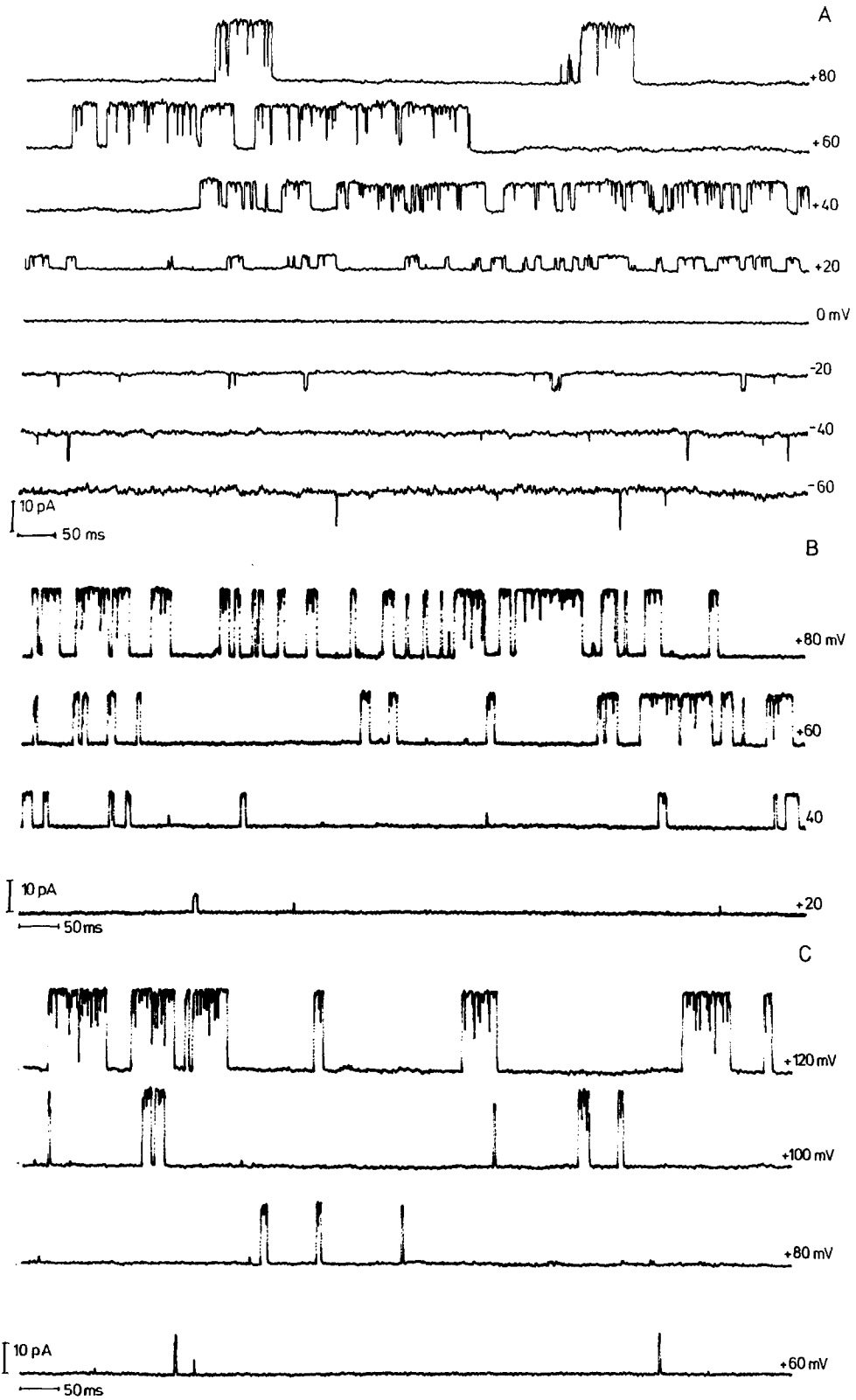

Fig. 5A–C. (Legend see page 53)

1 μM, 50 nM, and Ca^{2+}-free, estimated to be $\sim 10^{-9}$ M, are shown in Fig. 5 A–C, respectively. In Fig. 5A at 1 μM Ca^{2+}, kinetic behaviour very much resembles that seen with the unbuffered pipette solution in Fig. 3B, except that at any given potential, the open event lifetimes are somewhat shorter. In Figs. 5B and 5C it is apparent that both lifetime and frequency of the open events decrease as $[Ca^{2+}]$ is reduced. However, because the duration of the bursts at positive potentials increases as $[Ca^{2+}]$ is reduced, the total activity of the channel seems to be greater than at the higher calcium levels. The whole kinetic scheme appears to be shifted along the voltage axis by the change in the calcium concentration. This impression is confirmed in Fig. 6, where the equilibrium constant K, determined as described under 'methods' by the counting of open state and closed state data points as $K = P_o/(1\text{-}P_o)$, is plotted on a logarithmic scale against the membrane potential for several calcium concentrations.

It should perhaps be pointed out that not all the channels that we have observed fit into Fig. 6 well. In about 40% of the cases, the points follow a line with approximately the same slope, but shifted to the left by roughly 30 mV from the corresponding data for the regular channels at the same $[Ca^{2+}]$. It is unclear whether these cases actually represent a different population of channels, or merely indicate a locally increased calcium concentration due perhaps to the proximity of calcium channels or to unspecific membrane leaks or damage. Data points from such channels scatter much more than from regular channels, suggesting that the latter interpretation may be correct. From the slope of the data in Fig. 6 one can determine the amount of energy involved in the voltage dependent gating of the channels according to the relation $K \sim \exp(a \cdot F/RT \cdot (V-V^*))$. The value of the slope in each case is close to $2.0 \cdot F/RT$. From this we can infer that the voltage dependent gating process involves the transfer of the equivalent of two elementary charges across the membrane, or of a larger charge across a correspondingly smaller potential difference. In Fig. 7 the values from Fig. 6 at 60 mV are shown as a function of the nominal $[Ca^{2+}]$ on a double logarithmic plot, together with the slopes $a = 1$ and $a = 2$ for reference.

In Fig. 8 A and B the open and closed mean lifetimes, as determined from the actual event lifetime distributions, are plotted as a function of the membrane potential for the various calcium concentrations. As pointed out, these data, which are derived from the actual lifetime evaluation as discussed under 'methods', scatter more than the P_o values, even from one record to the next within one experiment. This may be to some extent due to the problems involved in eliminating the flickers, as discussed. However, a more fundamental reason may be that the actual event lifetimes do not depend on the energy difference between the open and closed states, as the equilibrium constant K does, but on the activation energies of the transition processes. They may therefore be

---

Fig. 5A–C. Typical fluctuations of the Ca^{2+} dependent K^+ channel at various internal calcium concentrations. Outside solution: potassium bath solution. Pipettes were filled with EGTA-calcium buffers (see Table 1). Nominal calcium concentrations are **A** 1 μM, **B** 50 nM, **C** ~ 1 nM

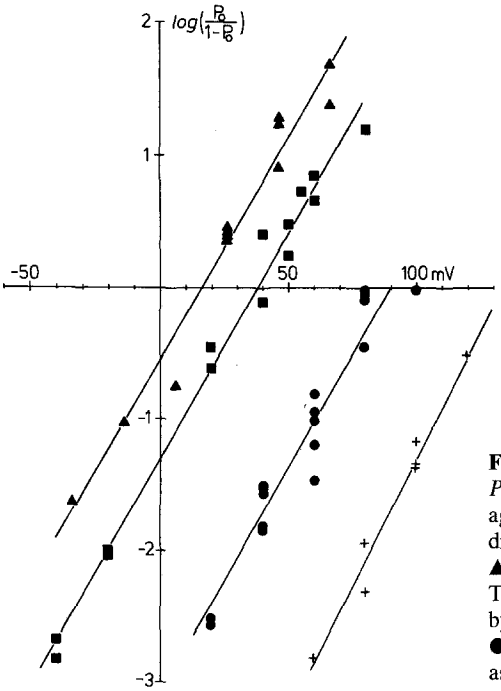

Fig. 6. The equilibrium constant K = $P_o/(1\text{-}P_o)$ plotted on a logarithmic scale against the membrane potential for four different internal calcium concentrations: ▲ 2 μM; ■ 1 μM; ● 50 μM; + ~ 1 nM. The slopes in terms of *F/RT* determined by linear regression are ▲ 1.97; ■ 1.99; ● 2.01 and + 2.28. Experimental conditions as in Fig. 5

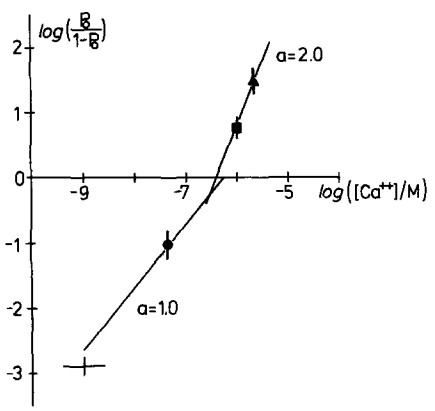

Fig. 7. The values of K, taken from Fig. 6 at 60 mV, plotted against the calcium concentration. Slopes of 1.0 and 2.0 are indicated for reference

expected to depend much more sensitively on the temperature, the lipid environment, and other parameters than the equilibrium value of K derived from P_o. That the scatter is indeed due to such external parameters rather than to errors in the evaluation procedure is suggested by the fact that the consistency test, Eq. (43), gives quite good results unless the number of events is very small or their duration very short compared to the time resolution of the equipment.

Figures 9 A and B again show the values from Figs. 8 A and B taken at 60 mV as a function of calcium concentration, with slopes of 1.0 and −1.0 indicated for orientation.

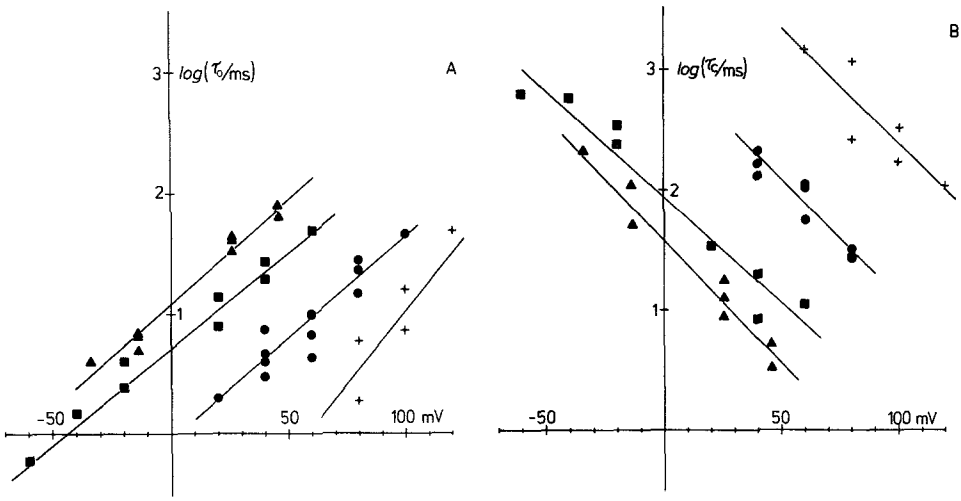

Fig. 8A and B. The time constants for the open state τ_o (A) and for the closed state τ_c (B) are plotted as a function of membrane potential. Calcium concentrations are as in Fig. 6. The slopes in terms of F/RT were found by linear regression and are 1.02, 0.93, 0.99 and 1.43 for the open state lifetimes and −1.18, −1.03, −1.13 and −1.10 for the closed states, in order of decreasing $[Ca^{2+}]$

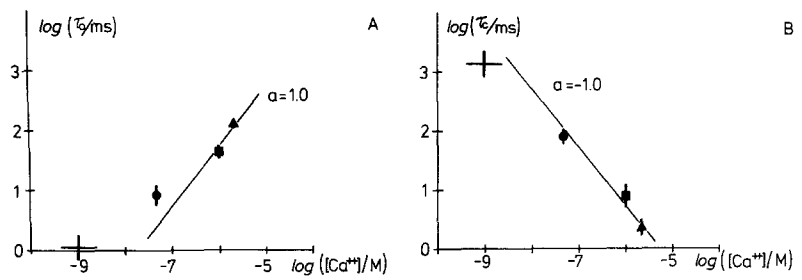

Fig. 9A and B. The values of log τ_o (A) and log τ_c taken from Fig. 8A and B at 60 mV are plotted against the calcium concentration. Slopes of 1.0 or −1.0 are shown for reference

Discussion

From the voltage dependence of the apparent equilibrium constant $K = P_o/(1\text{-}P_o)$ in Fig. 6 one cannot conclude which one of the models gives the best description of the channels. The activation model (A) does not predict a voltage dependence, and if there is any it should be uncoupled from the agonist sensitivity. The attraction of the blocking models (B, C) is that the closely parallel effect of membrane potential and internal $[2^{2+}]$ on the channel is clearly predicted by Eqs. (30) and (41). This is plausible because the closing of the channel is effected by the gate, and can be hindered either by calcium ions or by sufficiently positive potentials. The blocking models therefore appear to be somewhat more attractive on the basis of Fig. 6. The slope of the regression lines is close to 2.0 · F/RT, which means that the gating process involves the transfer

of the equivalent of two elementary charges across the membrane potential. This reflects the entry of the charged gate into the channel. The sign of the voltage dependence is consistent with a negatively charged gate acting from the inside, as postulated by the models (B, C). From the calcium dependence of K shown in Fig. 7 one again cannot decide conclusively which model is best because at calcium concentrations ~1 μM all three models make the same prediction $K \sim [Ca^{2+}]^2$ (Eqs. 19, 28 and 39).

In order to clearly differentiate between the models we must turn to the actual open and closed lifetimes plotted in Figs. 8 and 9. Figures 8 A and B show that the open and closed state time constants (τ_o, τ_c) both depend on the membrane potential with slopes of approximately +1 and −1, respectively, in the semilogarithmic presentation. This is consistent with the view that a charged structure, i.e., the gate, jumps back and forth across a symmetrical barrier within the channel. The high selectivity of the channel for K^+ over Na^+, concomitantly with the high conductance value of 240 pS in the presence of symmetrical K^+ points to a specific selectivity filter of short length within the channel. Presumably this narrow pathway is locked and unlocked by the gate.

The real difference between the three models is in their predictions for the open and closed state lifetimes as a function of $[Ca^{2+}]$. For the activation model we have (Eqs. 16, 18): $\tau_o = \text{const}$, $\tau_c \sim [Ca^{2+}]^{-2}$. The blockade model yields (Eqs. 23, 27): $\tau_o \sim [Ca^{2+}]^2$, $\tau_c = \text{const}$, whereas the combined activation/blockade mechanism predicts (Eqs. 35, 37): $\tau_o \sim [Ca^{2+}]$, $\tau_c \sim [Ca^{2+}]^{-1}$, for $[Ca^{2+}]$ concentrations around 1 μM. In Fig. 9 we actually find a slope of approximately +1 for the open lifetimes and of −1 for the closed lifetimes, which clearly favors the activation/blockade mechanism over the other proposed models.

A second prediction of the combined model is the existence of a high affinity binding site for Ca^{2+}. Therefore, the calcium concentration dependence of K and τ_o should be reduced at $[Ca^{2+}]$ below the value of the binding constant. Data points in Figs. 7 and 9A seem to indicate that K becomes linearly dependent, and τ_o independent, of $[Ca^{2+}]$ at $[Ca^{2+}] < 10^{-7}$ M. Therefore, as a rough estimate, $L \approx 10^{-7}$ M.

Calcium could also modify a voltage-dependent channel via changes in the membrane surface charge density. However, the semilogarithmic equivalence relation (Eq. 41) cannot be explained by a surface charge effect. Also, as lipid bilayer experiments show, such effects would not be expected in the μM $[Ca^{2+}]$ range.

Although several authors have reported single Ca^{2+} dependent K^+ channels (Marty 1981; Lux et al. 1981; Palotta et al. 1981), up to now only two attempts at a statistical analysis of these channels have been published (Latorre et al. 1982; Barrett et al. 1982). Since both have evaluated the open state probability but not the lifetimes of the open and closed events themselves, their data cannot be used to determine which of the models is correct. It is nevertheless instructive to compare their data with ours.

The channels investigated by Latorre et al. (1982) originate from rabbit T-tubular vesicles and may therefore differ from our myoball channels. Their behaviour, however, with respect to voltage and $[Ca^{2+}]$ dependence is very similar.

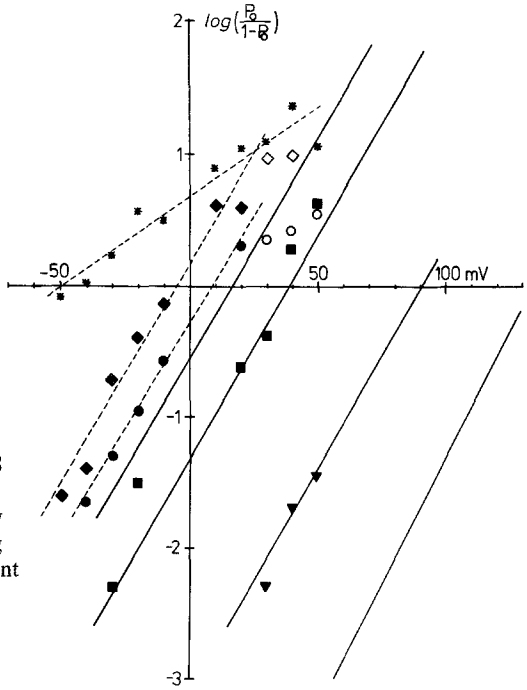

Fig. 10. Data from Fig. 8C of Barrett et al. (1982) replotted as log (P_o/1-P_o) for [Ca^{2+}] of 100 μM (*); 10 μM (◆); 5 μM (●); 1 μM (■); and 0.1 μM (▼). Data can be fitted as shown with slopes of 0.8 for 100 μM Ca^{2+}, 1.96 for 10 μM and 2.09 for 5 μM, all in units of *F/RT*. Only solid points were included in determining these slopes whereas open points represent data which we consider too low because of desensitization. Our own regression fits from Fig. 6 (this paper) are shown as heavy lines

The definition of the open state probability within bursts $f(V)$ of Latorre et al. (1982) is the same as our P_o and data can be compared directly. The voltage dependence of $K = f(V)/(1\text{-}f(V))$ ($= P_o/(1\text{-}P_o)$ in our nomenclature) is well fitted by a straight line with a slope of $a \cdot F/RT$ in a semilogarithmic plot. The values $a = 2.3$, 2.1 and 2.0 at 3, 15 and 100 μM Ca^{2+}, respectively, agree well with our results. Since Latorre et al. (1982) do not show the dependence on [Ca^{2+}] explicitly, we have replotted their data for two potentials against the calcium concentration in Fig. 11. By a least squares fit to the data points we obtain an approximately quadratic dependence on [Ca^{2+}], again in agreement with our results and supporting the idea that two Ca^{2+} ions are required to open the channel. However,the channels from rabbit T-tubular vesicles appear to have a lower affinity for Ca^{2+} (or a larger value for the reference voltage V^*, see Eq. 39, 40) than those from embryonic rat muscle cells. Like us, Latorre et al. (1982) have not evaluated the bursting behaviour ('slow process') of the channels quantitatively, but their qualitative description agrees well with ours. Furthermore, in Fig. 4 of Latorre et al. (1982), both τ_o and τ_c clearly depend on the calcium concentration. Thus, we conclude that this channel is very similar to ours and can probably be described in the same way.

Since the work of Barrett et al. (1982) was done on rat myotubes, we should expect even better agreement between their data and ours than with those of Latorre et al. (1982). Unfortunately, in determining the open state probability P_o Barrett et al. (1982) did not discriminate between the long desensitized and the regular channel closures. Therefore their data deviate from ours whenever

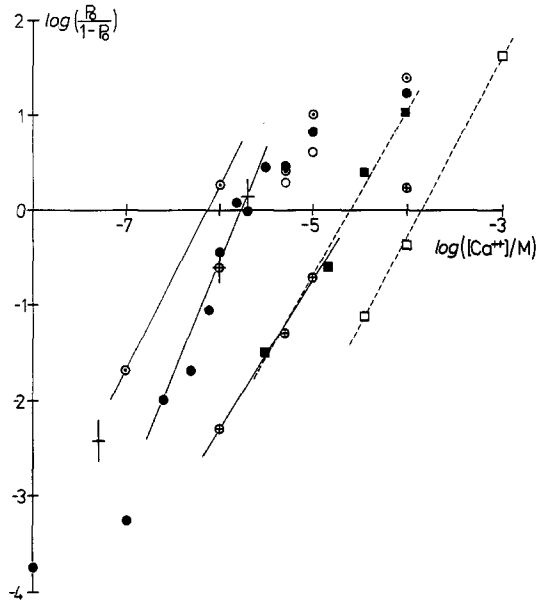

Fig. 11. Dependence of $P_o/(1\text{-}P_o)$ on Ca^{2+} from Barrett et al. (1982) and Latorre et al. (1982). The slope of a least squares fit (broken lines) for the data of Latorre et al. is 1.88 at +20 mV (□) and 1.74 at +60 mV (■). For the data of Barrett et al. at +20 mV (●) we find a slope of 2.47 with the values ≥ 5 μM Ca^{2+} not included. Full circles represent values from Fig. 6, and open circles from Fig. 8C of Barrett et al. For the data from Fig. 8C of Barrett et al. at +40 mV (⊙) and −30 mV (⊕) we find slopes of 1.96 and 1.56, respectively. Our own data are represented by the averaged values at +20 mV taken from Fig. 8 of this paper (+)

appreciable desensitization occurs. To facilitate comparison, we have replotted the data of Barrett et al. (1982) in terms of $K = P_o/(1\text{-}P_o)$ in Figs. 10 and 11. It is apparent that, within experimental scatter, the data points from Barrett et al. (1982) coincide with ours quite well with the restriction that their values at higher $[Ca^{2+}]$ and potentials deviate strongly towards lower values. We believe that this is due to the effect of desensitization.

In Fig. 10, straight lines fitted to the date of Barrett et al. (1982) yield slopes of approximately $2 \cdot F/RT$ at all potentials and Ca^{2+} concentrations where desensitization is not important, as it is the case for our K data determined within bursts under all conditions. This indicates that the same channel has been investigated in both cases, and that the choice of outside-out versus inside-out patch configuration does not affect the quantitative results.

For the $[Ca^{2+}]$ dependence of P_o at +20 mV Barrett et al. (1982) calculate a slope of 2.77 on a double logarithmic plot, suggesting a third power relationship. To resolve this discrepancy, we have included their data for three potentials in Fig. 11. Instead of P_o, which of course levels off to 1.0 at sufficiently high potentials and $[Ca^{2+}]$, we have again plotted the more meaningful quantity $K = P_o/(1\text{-}P_o)$. Data points for $[Ca^{2+}] \geq 5$ μM should not be included in determining the slope, because they seem to be depressed by desensitization. The slope of a least squares approximation yields 2.47. Since the slopes at other potentials in Fig. 11 are close to 2 (+40 mV) or even less than 2 (−30 mV), we believe the data of Barrett et al. (1982) to be consistent with a second power relationship.

Because it is much larger than expected from the other data, Barrett et al. (1982) suggest that their P_o value at 0.01 μM Ca^{2+} (see Fig. 11) is due to a 'background' activity originating from some other gating mechanism. However,

the value found is in agreement with the reduction of slope predicted by our model (C) for calcium concentrations comparable with and below the binding constant of the gate. In our view, it is therefore not necessary to subtract the value for 0.01 μM Ca^{2+} from the other values before determining the slope. However, the values at 0.01 and 0.1 μM [Ca^{2+}] lie in a region where the channel is open less than 0.1% of the time and data are subject to extreme scattering. Just as with our own data we have therefore excluded these points from regression.

We have shown that Ca^{2+} dependent K^+ channels from rat myoballs can be described by an activation/blockade mechanism involving two negatively charged binding sites for Ca^{2+}. One site, with a low affinity for Ca^{2+}, is situated near the channel entrance. The other site is associated with a charged gate that normally blocks the channel. This model is in contrast to the view of an agonist activated channel that is generally accepted for this and other channels. However, the idea of a charged gate or 'plug' is not an unreasonable one. Miller and Rosenberg (1979) have presented convincing evidence for a movable charged gate structure on K^+ channels from sarcoplasmic reticulum, whose voltage dependence could be removed by enzymatic treatment. It may therefore well be that other channels can also be described by an activation/blockade mechanism. In case of an uncharged gate the blockade reaction would of course be voltage independent.

We therefore briefly look at other 'agonist-activated' channels. There are many surprising similarities between the various kinds of ion channels that have been investigated by the patch clamp technique. Two agonist molecules seem to be required for activation (Adams 1981; Sakmann et al. 1982), and most channels appear to show the brief 'flickering' closures of the open state (Colquhoun and Sakmann 1981; Cull-Candy and Parker 1982). In the membrane at rest, the intensively studied nicotinic acetylcholine receptor exhibits a state of low affinity for the agonist whereas at equilibrium acetylcholine stabilizes a high affinity state (Heidmann and Changeux 1978). This behaviour is reminiscent of our model (C) in that the binding of the agonist at the low affinity site apparently exposes the high affinity site, probably by allosteric interactions. Interesting evidence also comes from investigations of the glutamate receptor channel from locust muscle. Whereas Cull-Candy et al. (1981) found the open state lifetime of these channels to be virtually independent of the agonist concentration up to 1,000 μM, Gration et al.(1981) showed that the open state lifetime increases with higher concentrations of glutamate in an approximately linear manner. Instead of binding sites with variable affinity, a glutamate-sensitive blocking gate with a binding constant near 1 mM might also reconcile these results. It is possible that different kinds of ion channel proteins are evolutionally related. In that case, one would expect extensive structural similarities between them. Thus,they may all have a common structure involving a blocking gate, but differ in the binding sites responsible for ion selectivity and agonist recognition. To answer these questions, much further work must be done.

Acknowledgements. We gratefully acknowledge the help and advice of Dr. B. Sakmann in whose laboratory the work started. This work was supported by the Deutsche Forschungsgemeinschaft (SFB 114).

References

Adams PR (1981) Acetylcholine receptor kinetics. J Membrane Biol 58: 161–174
Adams PR, Constanti A, Brown DA, Clark RB (1982) Intracellular Ca^{2+} activates a fast voltage-sensitive K^+ current in vertebrate sympathetic neurones. Nature 296: 746–749
Barrett JN, Magleby KL, Pallotta BS (1982) Properties of single calcium-activated potassium channels. J Physiol (in press)
Boheim G, Methfessel C, Sakmann B (1982) Ca^{++} activates K^+ channel by preventing channel blockade. Pflügers Arch 392: R19
Colquhoun D, Hawkes AG (1977) Relaxation and fluctuations of membrane currents that flow through drug operated channels. Proc R Soc London B199: 231–262
Colquhoun D, Sakmann B (1981) Fluctuations in the microsecond time range of the current through single acetylcholine receptor ion channels. Nature 294: 464–466
Cull-Candy SG, Miledi R, Parker I (1981) Single glutamate-activated channels recorded from locust muscle fibres with perfused patch-clamp electrodes. J Physiol 321: 195–210
Cull-Candy SG, Parker I (1982) Rapid kinetics of single glutamate-receptor channels. Nature 295: 410–412
Fink R, Hase S, Lüttgau HC, Wettwer E (1983) The effect of cellular energy reserves and internal Ca^{++} on the potassium conductance in skeletal muscle of the frog. J Physiol (in press)
Gration KAF, Lambert JJ, Ramsey R, Usherwood PNR (1981) Nonrandom openings and concentration-dependent lifetimes of glutamate-gated channels in muscle membrane. Nature 291: 423–425
Hagiwara S, Nakajima S (1966) Effects of the intracellular Ca ion concentration upen the excitability of the muscle fiber membrane of a Barnacle. J Gen Physiol 49: 807–818
Hamill OP, Marty A, Neher E, Sakmann B, Sigworth FJ (1981) Improved patch-clamp techniques for high-resolution current recording from cells and cell-free membrane patches. Pflügers Arch 391: 85–100
Heidmann T, Changeux JP (1978) Structural and functional properties of the acetylcholine receptor protein in its purified and membrane-bound states. Annu Rev Biochem 47: 317–357
Katz B (1966) Nerve, muscle and synapse. McGraw-Hill, New York
Kemeny JG, Snell JL (1976) Finite Markov chains. Springer, Berlin Heidelberg New York
Latorre R, Vergara C, Hidalgo C (1982) Reconstitution in planar lipid bilayers of a Ca^{2+}-dependent K^+ channel from transverse tubule membranes isolated from rabbit skeletal muscle. Proc Natl Acad Sci USA 79: 805–810
Lux HD, Neher E, Marty A (1981) Single channel activity associated with the calcium dependent outward current in helix pomatia. Pflügers Arch 389: 293–295
Marty A (1981) Ca-dependent K channels with large unitary conductance in chromaffin cell membranes. Nature 291: 497–500
Meech RW (1978) Calcium-dependent potassium activation in nervous tissues. Annu Rev Biophys Bioeng 7: 1–18
Miller C, Rosenberg R (1979) Modification of a voltage-gated K^+ channel from sarcoplasmic reticulum by a pronase-derived specific endopeptidase. J Gen Physiol 74: 457–478
Neher E, Sakmann B, Steinbach JH (1978) The extracellular patch clamp: A method for resolving currents through individual open channels in biological membranes. Pflügers Arch 375: 219–228
Neher E, Steinbach HJ (1978) Local anaesthetics transiently block currents through single acetylcholine-receptor channels. J Physiol 277: 153–176
Pallotta BS, Magleby KL, Barrett JN (1981) Single channel recordings of Ca^{2+} activated K^+ currents in rat muscle cell culture. Nature 293: 471–474
Sakmann B, Hamill OP, Bormann J (1982) Activation of chloride channels by putative inhibitory transmitters in spinal cord neurons. Pflügers Arch 392: R19
Sakmann B, Patlak J, Neher E (1980) Single acetylcholine-activated channels show burst-kinetics in presence of desensitizing concentrations of agonist. Nature 286: 71–73
Schwarz W, Passow H (1983) Ca-activated K^+ channels in erythrocytes and excitable cells. Annu Rev Physiol (in press)

Received June 4, 1982/Accepted July 7, 1982